

---

---

PHYSICAL PROPERTIES  
OF CRYSTALS

---

---

## Raman Scattering of Light in Diamond Microcrystals

V. S. Gorelik<sup>a,b,\*</sup>, A. V. Skrabatun<sup>a,b</sup>, and Dongxue Bi<sup>a,b</sup>

<sup>a</sup> Lebedev Physical Institute, Russian Academy of Sciences, Moscow, 119991 Russia

<sup>b</sup> Bauman Moscow State Technical University, Moscow, 105005 Russia

\*e-mail: gorelik@sci.lebedev.ru

Received August 27, 2018; revised September 5, 2018; accepted September 17, 2018

**Abstract**—Raman spectra of monodisperse crystalline diamond powders have been studied in dependence of the sample sizes. Raman scattering was excited by a near-IR cw laser ( $\lambda_0 = 785$  nm), which ensured suppression of the photoluminescence signal. Powders consisting of close-packed particles in the form of nanodiamonds (0.2–0.3  $\mu\text{m}$  in size) and microdiamonds of specified sizes (up to 180  $\mu\text{m}$ ) have been studied. The recorded Raman spectra of the microdiamond powders are characterized by anomalously high intensity, which is related to the excitation radiation trapping in microparticles, the size of which exceeds significantly the lasing wavelength. The Raman spectra contain a sharp line at a frequency of  $1332\text{ cm}^{-1}$  and additional bands in the vicinity of fundamental-mode overtones.

DOI: 10.1134/S106377451903009X

### INTRODUCTION

Many researchers have been engaged in investigations of regularities of Raman scattering in diamond crystals; these studies began almost immediately after the discovery of this phenomenon [1–5]. The objects of study were samples of natural [1, 2, 6] and synthetic [6–8] diamonds. A characteristic feature of the Raman spectrum of a diamond crystal is the presence of only one strong first-order line at a frequency of  $1332\text{ cm}^{-1}$ . Upon an increase in the excitation-radiation intensity, additional satellites related to two-phonon states arise in the scattered-radiation spectrum [9, 10]. Currently, an urgent problem is to establish the regularities of Raman spectra from nano- and microcrystals [11–16]. Thin diamond films (thickness of 1–50  $\mu\text{m}$ ) grown by chemical vapor deposition (CVD) were investigated previously [17–19]. In contrast to bulk crystals,  $\sim 1\text{-}\mu\text{m}$ -thick diamond films exhibited additional bands in the range of  $400\text{--}3000\text{ cm}^{-1}$  [18]. Preparation of cubic diamond microparticles 10–100  $\mu\text{m}$  in size was described in [13]. These microparticles were formed in a concentrated gaseous phase at the thermal graphite activation with a subsequent deposition of crystals on a substrate. Raman spectra of diamond microparticles 0.1–2.0  $\mu\text{m}$  in size upon excitation by an argon laser ( $\lambda_0 = 457.9$  and  $514.5\text{ nm}$ ) were studied in [11]. Investigations were carried out only for the fundamental mode  $\nu = 1332\text{ cm}^{-1}$ . A broadening of the corresponding Raman line with a decrease in the microcrystal size was observed.

In the IR region, the diamond spectra were analyzed by comparing with the density of phonon states

and shapes of the dispersion curves calculated in [4–6, 20, 21]. The results of calculating the curves of the densities of one- and two-phonon states and their comparison with the second-order Raman spectra were reported in [9, 10].

The purpose of this study was to establish the regularities in the Raman spectra of monodisperse diamond powders in dependence of the particle size in the range of 0.2–180  $\mu\text{m}$ . We analyzed the possibility of using powders consisting of diamond plates as optical microcavities enhancing the interaction efficiency between electromagnetic radiation and material.

### EXPERIMENTAL

Preforms for microdiamonds were made of graphite by static compression at a high temperature (1000–3000°C) and an ultrahigh pressure (5–10 GPa). Experimental samples were monodisperse microdiamond powders with a mean particle size from 0.2 to 180  $\mu\text{m}$ . We used nine sets of crystalline powders with specified particle sizes: 0.2–0.3, 1, 3.5–4.2, 6.5–7.3, 28–32, 43–48, 56–64, 65–73, and 150–185  $\mu\text{m}$ . Diamond microparticles were shaped as plane-parallel plates (Fig. 1).

The experimental setup for exciting and recording spontaneous Raman scattering spectra was described in [22]. The excitation source is a 100-mW laser with a wavelength  $\lambda_0 = 785\text{ nm}$ ; the spectral resolution is  $1\text{ cm}^{-1}$ .

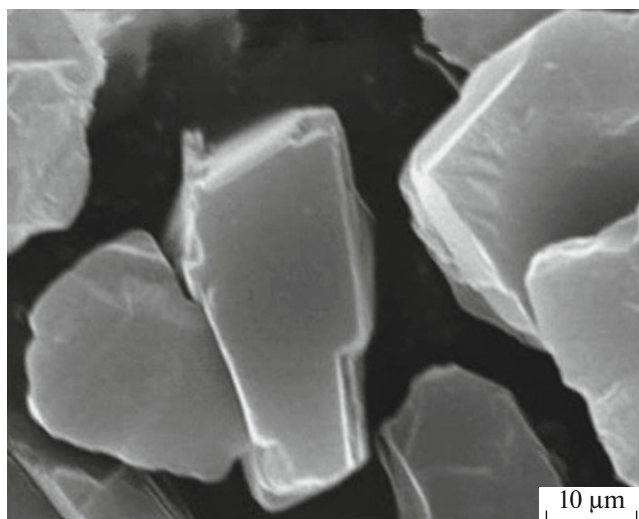


**Fig. 1.** Photographs of crystals in the microdiamond powder.

## RESULTS

Raman spectra of monodisperse microdiamond powders of different sizes are shown in Fig. 2. All spectra were recorded at an exposure of 10 s. The observed Raman spectra of microdiamond powders (Fig. 2) contain several bands. The diamond single-photon scattering line at a frequency  $\nu = 1332 \text{ cm}^{-1}$  is the strongest. The half-width of this line is  $\Delta\nu = 2 \text{ cm}^{-1}$ . Observation of a narrow line at a frequency  $\nu = 1332 \text{ cm}^{-1}$  confirms the presence of diamond crystalline phase in the samples under study. The Raman spectra of diamond crystallites less than  $1 \mu\text{m}$  in size (Figs. 2a, 2b) exhibit intense background in the entire spectral region, which decays with an increase in the frequency shift. The continuous background sharply decreases with an increase in the microcrystal size from 1 to  $60 \mu\text{m}$ , and the Raman intensity at the fundamental mode of  $1332 \text{ cm}^{-1}$  increases with respect to the background (Figs. 2c–2i). Note that there are numerous pulsations in the vicinities of 96, 194, 269, 365, 478,

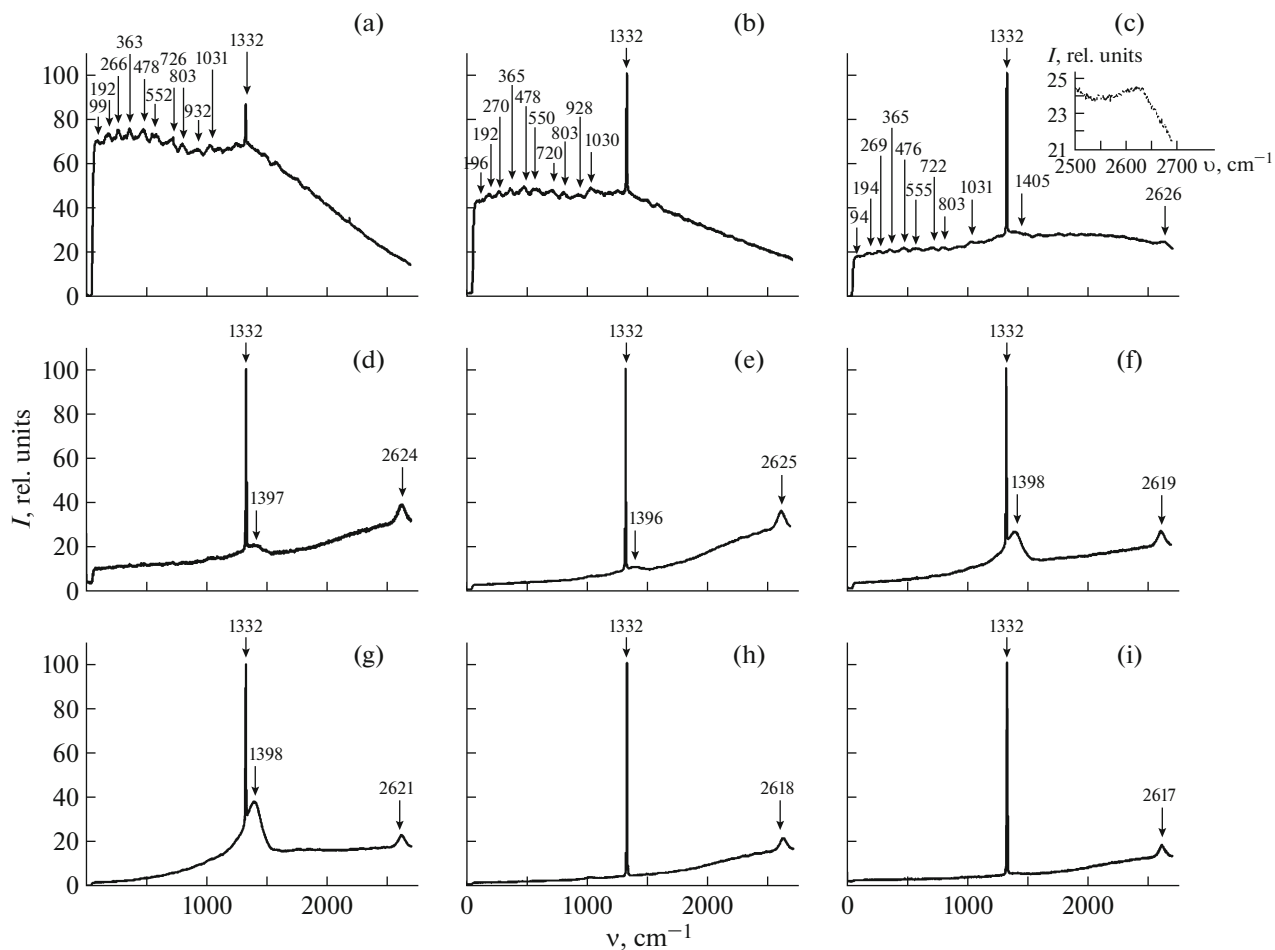


**Fig. 2.** Raman spectra of microdiamond powders of different sizes: (a) 0.2–0.3, (b) 1, (c) 3.5–4.2, (d) 6.5–7.3, (e) 28–32, (f) 43–48, (g) 56–64, (h) 65–73, and (i) 150–180  $\mu\text{m}$ . The Raman spectral region in the vicinity of the band  $\nu = 2626 \text{ cm}^{-1}$  is shown in the inset in Fig. 2c.

555, 722, 803, 932, and 1031  $\text{cm}^{-1}$  in the low-frequency Raman spectral region for (0.2–4.2)- $\mu\text{m}$  microdiamonds (Figs. 2a–2c). The Raman spectra of diamond microparticles of larger sizes does not exhibit any low-frequency pulsations. The intensity of the Raman spectra of the monodisperse microdiamond powders under study is much higher (by one–two orders of magnitude) than that for some other inorganic materials ( $\text{NaNO}_2$ ,  $\text{KIO}_3$ , etc.). Beginning with the microdiamond size of 3.5  $\mu\text{m}$ , a wide band peaking near 2620  $\text{cm}^{-1}$  manifests itself in the second-order Raman spectral region (Figs. 2c–2i). Figures 2c–2g for (3.5–64)- $\mu\text{m}$  microdiamonds also exhibit a wide band near  $\nu = 1400 \text{ cm}^{-1}$ . Its intensity increases with an increase in the mean microcrystal size and attains a maximum at 56–64  $\mu\text{m}$ . With a further increase in the diamond-powder microparticle size, no bands are observed in this frequency range.

## DISCUSSION

Diamond, being the main high-pressure carbon phase, is crystallized in the cubic system ( $O_h^7$ ,  $Z = 2$ ) with tetrahedral arrangement of C–C bonds around each carbon atom [8]. The fact that the diamond lattice is homonuclear, along with its high symmetry, determines the simplicity of a vibrational spectrum. According to the results of the group-theoretical analysis, the total spectrum of optical lattice vibrations of the diamond crystal has the form  $T_{\text{opt}} = F_{2g}$ . The corresponding vibration is allowed in Raman spectra. The frequency of this mode in the first-order Raman spectrum corresponds to  $\nu = 1332 \text{ cm}^{-1}$  (Fig. 2). The manifestation of this vibration in the first-order IR spectrum for diamond is forbidden by the selection rules. The parameters of this mode for a structurally perfect diamond lattice were investigated in detail in a wide temperature range [6]. The theory [11, 12] predicts that a decrease in the diamond crystal sizes should deform the fundamental line profile in the Raman spectrum and reduce its frequency.

The diamond microcrystallites contained in the powders under investigation were shaped as plane-parallel plates (Fig. 1). As is known [9], diamond crystals are characterized by a high refractive index ( $n = 2.4$ – $2.5$  in the visible range). When excitation radiation with a wavelength smaller than the microparticle size enters these structures, it may be trapped as a result of multiple reflections from the boundaries of the corresponding microcavities. This leads to an increase in the Raman scattering intensity (Raman opalescence effect) in diamond microcrystals, which is observed in the above-described experiments (Fig. 2). A similar cavity effect can be implemented for acoustic and optical phonons corresponding to the Brillouin-zone critical points (Table 1). Accordingly, one would

**Table 1.** Frequencies of critical points ( $\Gamma$ , X, K, L, and W) of the phonon branches of diamond crystal

Critical points of the Brillouin zone	Phonon branches	Phonon frequencies at critical points, $\text{cm}^{-1}$	
		[21]	[6]
$\Gamma$	–	$1332.5 \pm 1$	$1332.5 \pm 0.5$
X	LO, LA	$1191 \pm 3$	$1185 \pm 5$
	TO	$1072 \pm 2$	$1069 \pm 5$
	TA	$829 \pm 2$	$807 \pm 5$
K	LO	$1239 \pm 2$	$1230 \pm 5$
	TO	$1111 \pm 1$	$1109 \pm 5$
	TO	$1042 \pm 2$	$1045 \pm 5$
	LA	$992 \pm 3$	$988 \pm 5$
	TA	$978 \pm 1$	$980 \pm 5$
	TA	$764 \pm 4$	–
L	LO	$1256 \pm 4$	$1252 \pm 5$
	TO	$1220 \pm 2$	$1206 \pm 5$
	LA	$1033 \pm 2$	$1006 \pm 5$
	TA	$553 \pm 2$	$563 \pm 5$
W	LO, LA	$1146 \pm 1$	$1179 \pm 5$
	TO	$1019 \pm 3$	$999 \pm 5$
	TA	$918 \pm 12$	$908 \pm 5$

LO and TO are, respectively, the longitudinal and transverse optical phonons and LA and TA are, respectively, the longitudinal and transverse acoustic phonons.

expect the intensity of some bands corresponding to the second-order processes (overtone or complex tones) to increase in the Raman spectrum of diamond microcrystals. In this context, the band at a frequency of 2620  $\text{cm}^{-1}$  can be assigned to the fundamental-mode overtone 1332  $\text{cm}^{-1}$ . The intensity of this band is only 4–5 times lower than that of the fundamental Raman line at a frequency of 1332  $\text{cm}^{-1}$ . The observed frequency shift ( $\Delta = 42 \text{ cm}^{-1}$ ) corresponds to the binding energy of the biphonon generated under these conditions [23]. In bulk diamond crystals, the intensity of the second-order Raman bands is much lower (by two orders of magnitude) than that of the 1332- $\text{cm}^{-1}$  fundamental mode [8].

Thus, the conditions for biphonon formation upon the Raman scattering excitation in diamond microcrystals of specified sizes are preferred as compared to those for bulk single crystals. In a bulk diamond single crystal, the overtone frequency (2668  $\text{cm}^{-1}$ ) is close to

the doubled fundamental-tone frequency ( $1332\text{ cm}^{-1}$ ); i.e., the biphonon has a very low binding energy and rapidly decays. The observed interference intensity pulsations (Figs. 2a–2c) at frequencies of 555, 722, 803, 932, and  $1031\text{ cm}^{-1}$  in (0.2–4.2)- $\mu\text{m}$  diamond crystals can be explained by the microcavity effect for the phonons corresponding to the internal region or the boundary of the Brillouin zone (Table 1). Raman spectra of  $\sim 1\text{-}\mu\text{m}$ -thick diamond CVD films were recorded in [18] upon laser excitation with a wavelength  $\lambda_0 = 785\text{ nm}$ . The  $1332\text{-cm}^{-1}$  fundamental line was barely observed in the Raman spectrum; however, additional sharp lines were found, which are likely due to the presence of impurities and lattice defects in the films studied.

Characteristic lines corresponding to the manifestation of biphonons were found previously in the second-order Raman spectra of some crystals [24–26]. These effects occur generally under the Fermi-resonance conditions, when the overtone (complex tone) frequency is close to the frequency of the fundamental vibration of the same symmetry type. In this case, the formation of biphonons can be explained by the microcavity effect, which sharply increases the density of two-phonon states for phonons of a certain type.

The band in the Raman spectra in the vicinity of  $1400\text{ cm}^{-1}$ , which is observed in microcrystals 3.5–64  $\mu\text{m}$  in size, is close to the doubled frequency of transverse acoustic phonons TA (Table 1) at the Brillouin zone boundary. Taking into account the decrease in the frequency due to the binding energy, this band can also be interpreted as the result of biphonon formation under the conditions of strong reflection of the corresponding waves from the microcavity boundaries. Note that no lines indicating the presence of graphite, graphene, nanotubes, or other carbon phases known in the literature were found in the recorded Raman spectra.

## CONCLUSIONS

The Raman spectra of diamond nano- and microcrystals 0.2–180.0  $\mu\text{m}$  in size, forming monodisperse diamond powders, were recorded. The diamond microcrystals present in the powder were shaped as plane-parallel plates (i.e., served as optical and acoustic cavities). The intensity of the  $1332\text{-cm}^{-1}$  fundamental mode in the microdiamond Raman spectra exceeds that of the Raman spectra of inorganic powders recorded under similar conditions by more than an order of magnitude. The reason is the multiple scattering of excitation radiation in diamond microcavities (whispering gallery mode), which can be classified as a Raman opalescence. This effect made it possible to record spontaneous Raman scattering spectra at very small exposures (1–10 s) using near-IR cw laser radiation ( $\lambda_0 = 785\text{ nm}$ ). The high efficiency of sponta-

neous Raman scattering in microdiamond powders allows one to observe low-threshold stimulated Raman scattering in them upon excitation by pulsed lasers [27].

It was found that, at certain microcrystal sizes, the Raman spectra contain second-order bands, which were interpreted as a manifestation of bound phonon (biphonon) states with a fairly high binding energy. The bound phonon states can be excited due to the increase in the density of two-phonon states because of multiple reflections of the corresponding waves from the microcavity boundaries. Thus, the use of diamond microcavities with specified sizes leads to significant modification of the optical and acoustic properties of diamond crystals and appears promising for observing various nonlinear optical phenomena: stimulated Raman scattering [27], nonlinear refraction, two-photon excited luminescence [28], etc.

## ACKNOWLEDGMENTS

This study was supported by the Russian Foundation for Basic Research (project nos. 16-08-00618, 16-02-00488, 18-02-00181, and 18-32-00259) and the China Scholarship Council.

## REFERENCES

1. R. Robertson and J. J. Fox, *Nature* **125**, 704 (1930).
2. R. S. Krishnan, *Proc. Indian Acad. Sci. A* **26**, 399 (1947).
3. D. Krishnamurt, *Proc. Indian Acad. Sci. A* **40**, 211 (1954).
4. H. M. J. Smith, *R. Soc.* **248**, 105 (1947).
5. G. Dolling and R. A. Cowley, *Proc. Phys. Soc.* **88**, 463 (1966).
6. S. A. Solin and A. K. Ramdas, *Phys. Rev. B* **1**, 1687 (1970).
7. F. P. Bundy, H. T. Hall, H. M. Strong, et al., *Nature* **176**, 51 (1955).
8. D. S. Knight and W. B. White, *J. Mater. Res.* **4**, 385 (1989).
9. A. M. Zaitsev, *Optical Properties of Diamond. A Data Handbook* (Springer, Berlin, 2001), p. 19.
10. W. Windl, P. Pavone, K. Karch, et al., *Phys. Rev. B* **48**, 3164 (1993).
11. M. Yoshikawa, Y. Mori, M. Maegawa, et al., *Appl. Phys. Lett.* **62**, 3114 (1993).
12. K. P. Argunov, V. S. Gorelik, B. I. Reznik, et al., *Kratk. Soobshch. Fiz. FIAN*, No. 9, 21 (1991).
13. A. V. Palmichenko, A. M. Jonasi, J. C. Charlier, et al., *Nature* **402**, 162 (1999).
14. L. Nasdala, S. Steger, and C. Reissner, *Lithos* **265**, 317 (2016).
15. V. V. Uglov, V. I. Shimanskii, D. P. Rusal'skii, et al., *Zh. Prikl. Spektrosk.* **75**, 524 (2008).

16. M. V. Tareeva, V. A. Antonov, V. P. Popov, et al., *Kratk. Soobshch. Fiz. FIAN*, No. 7, 40 (2017).
17. K. C. Lee, B. J. Sussman, M. R. Sprague, et al., *Nat. Photonics* **6**, 11 (2011).
18. P. W. May, J. A. Smith, and K. N. Rosser, *Diamond Relat. Mater.* **17**, 199 (2008).
19. M. G. Donato, G. Faggio, M. Marinelli, et al., *Eur. Phys. J. B* **20**, 133 (2001).
20. N. S. Vasil'ev and V. S. Gorelik, *Kratk. Soobshch. Fiz. FIAN*, No. 9, 15 (2011).
21. C. A. Klein, T. M. Hartnett, and C. J. Robinson, *Phys. Rev. B* **45**, 12854 (1992).
22. V. S. Gorelik, T. G. Golovina, and A. F. Konstantinova, *Crystallogr. Rep.* **64** (2), 287 (2019).
23. V. M. Agranovich and O. A. Dubovsky, *Int. Rev. Phys. Chem.* **5**, 93 (1986).
24. V. S. Gorelik, O. P. Maximov, G. G. Mitin, et al., *Solid State Commun.* **21**, 615 (1977).
25. G. G. Mitin, V. S. Gorelik, L. A. Kulevskii, et al., *Zh. Eksp. Teor. Fiz.* **68**, 1757 (1975).
26. V. Zh. Agranovich and I. I. Lalov, *Usp. Fiz. Nauk* **146**, 267 (1985).
27. O. Lux, V. G. Ralchenko, A. P. Bolshakov, et al., *Laser Phys. Lett.* **11**, 1 (2014).
28. S. N. Mikov, A. V. Igo, and V. S. Gorelik, *Fiz. Tverd. Tela* **41**, 1110 (1999).

*Translated by A. Sin'kov*